NASA/TM—2001-210986 IECEC2001–AT–11

Advanced Motor Control Test Facility for NASA GRC Flywheel Energy Storage System Technology Development Unit

Barbara H. Kenny
Glenn Research Center, Cleveland, Ohio

Peter E. Kascak
Ohio Aerospace Institute, Brook Park, Ohio

Heath Hofmann
Pennsylvania State University, University Park, Pennsylvania

Michael Mackin and Walter Santiago
Glenn Research Center, Cleveland, Ohio

Ralph Jansen
Ohio Aerospace Institute, Brook Park, Ohio

July 2001

The NASA STI Program Office . . . in Profile

Since its founding, NASA has been dedicated to the advancement of aeronautics and space science. The NASA Scientific and Technical Information (STI) Program Office plays a key part in helping NASA maintain this important role.

The NASA STI Program Office is operated by Langley Research Center, the Lead Center for NASA's scientific and technical information. The NASA STI Program Office provides access to the NASA STI Database, the largest collection of aeronautical and space science STI in the world. The Program Office is also NASA's institutional mechanism for disseminating the results of its research and development activities. These results are published by NASA in the NASA STI Report Series, which includes the following report types:

- TECHNICAL PUBLICATION. Reports of completed research or a major significant phase of research that present the results of NASA programs and include extensive data or theoretical analysis. Includes compilations of significant scientific and technical data and information deemed to be of continuing reference value. NASA's counterpart of peer-reviewed formal professional papers but has less stringent limitations on manuscript length and extent of graphic presentations.

- TECHNICAL MEMORANDUM. Scientific and technical findings that are preliminary or of specialized interest, e.g., quick release reports, working papers, and bibliographies that contain minimal annotation. Does not contain extensive analysis.

- CONTRACTOR REPORT. Scientific and technical findings by NASA-sponsored contractors and grantees.

- CONFERENCE PUBLICATION. Collected papers from scientific and technical conferences, symposia, seminars, or other meetings sponsored or cosponsored by NASA.

- SPECIAL PUBLICATION. Scientific, technical, or historical information from NASA programs, projects, and missions, often concerned with subjects having substantial public interest.

- TECHNICAL TRANSLATION. English-language translations of foreign scientific and technical material pertinent to NASA's mission.

Specialized services that complement the STI Program Office's diverse offerings include creating custom thesauri, building customized data bases, organizing and publishing research results . . . even providing videos.

For more information about the NASA STI Program Office, see the following:

- Access the NASA STI Program Home Page at ***http://www.sti.nasa.gov***

- E-mail your question via the Internet to help@sti.nasa.gov

- Fax your question to the NASA Access Help Desk at 301–621–0134

- Telephone the NASA Access Help Desk at 301–621–0390

- Write to:
  NASA Access Help Desk
  NASA Center for AeroSpace Information
  7121 Standard Drive
  Hanover, MD 21076

NASA/TM—2001-210986 IECEC2001–AT–11

Advanced Motor Control Test Facility for NASA GRC Flywheel Energy Storage System Technology Development Unit

Barbara H. Kenny
Glenn Research Center, Cleveland, Ohio

Peter E. Kascak
Ohio Aerospace Institute, Brook Park, Ohio

Heath Hofmann
Pennsylvania State University, University Park, Pennsylvania

Michael Mackin and Walter Santiago
Glenn Research Center, Cleveland, Ohio

Ralph Jansen
Ohio Aerospace Institute, Brook Park, Ohio

Prepared for the
36th Intersociety Energy Conversion Engineering Conference
cosponsored by the ASME, IEEE, AIChE, ANS, SAE, and AIAA
Savannah, Georgia, July 29–August 2, 2001

National Aeronautics and
Space Administration

Glenn Research Center

July 2001

Available from

NASA Center for Aerospace Information
7121 Standard Drive
Hanover, MD 21076

National Technical Information Service
5285 Port Royal Road
Springfield, VA 22100

Available electronically at http://gltrs.grc.nasa.gov/GLTRS

Proceedings of IECEC'01
36th Intersociety Energy Conversion Engineering Conference
July 29–August 2, 2001, Savannah, Georgia

IECEC2001-AT-11

ADVANCED MOTOR CONTROL TEST FACILITY FOR NASA GRC FLYWHEEL ENERGY STORAGE SYSTEM TECHNOLOGY DEVELOPMENT UNIT

Barbara H. Kenny[1] **Peter E. Kascak**[2] **Heath Hofmann**[3]

Michael Mackin[1] **Walter Santiago**[1] **Ralph Jansen**[2]

[1]NASA Glenn Research Center
21000 Brookpark Road
Cleveland, Ohio 44135

[2]Ohio Aerospace Institute
22800 Cedar Point Road
Brookpark, Ohio 44135

[3]Department of Electrical Engineering
Pennsylvania State University
University Park, Pennsylvania 16802

ABSTRACT

This paper describes the flywheel test facility developed at the NASA Glenn Research Center with particular emphasis on the motor drive components and control. A 4-pole permanent magnet synchronous machine, suspended on magnetic bearings, is controlled with a field orientation algorithm. A discussion of the estimation of the rotor position and speed from a "once around signal" is given. The elimination of small dc currents by using a concurrent stationary frame current regulator is discussed and demonstrated. Initial experimental results are presented showing the successful operation and control of the unit at speeds up to 20,000 rpm.

INTRODUCTION

One of the key components of the flywheel energy storage system is the electric motor and its control. Energy storage and recovery are achieved by using the motor to increase or decrease the flywheel rotor speed as necessary. Good control of the motor is thus very important for the proper operation of the flywheel system. As part of the flywheel technology development effort, NASA Glenn Research Center has built a test facility with the capability to rapidly test and evaluate advanced motor control algorithms. It is the purpose of this paper to describe the test facility (with particular emphasis on the motor control portion), the basic motor control algorithms developed and to present initial experimental results.

NOMENCLATURE

L_q is the q-axis machine inductance, henries.

L_d is the d-axis machine inductance, henries.

f^r_q q-axis voltage or current in the rotor reference frame.

f^r_d d-axis voltage or current in the rotor reference frame.

f^s_q q-axis voltage or current in the stator reference frame.

f^s_d d-axis voltage or current in the stator reference frame.

p is the derivative operator, d/dt.

θ_r is the angle between the stator q-axis and the rotor q-axis, radians.

λ_{af} is the flux linkage due to the rotor magnets, volt-sec.

ω_r is the electrical rotor speed, radians/second.

FLYWHEEL TEST FACILITY

The flywheel system test facility consists of a test cell and a control room. The test cell is physically separated from the control room for safety purposes. The present flywheel system under test consists of a 4 pole permanent magnet synchronous machine, a high strength composite rotor, magnetic bearings and a housing structure which is sealed and pumped to a low vacuum with water cooling capability. The flywheel system itself is housed in a containment structure that is closed during operation. Power for the motor is derived from a standard six switch three phase inverter with a dc power supply source. The inverter is a commercial off the shelf intelligent power module (gate drive circuitry included in the unit) rated at 600 volts, 200 amps and uses IGBTs for the power switches.

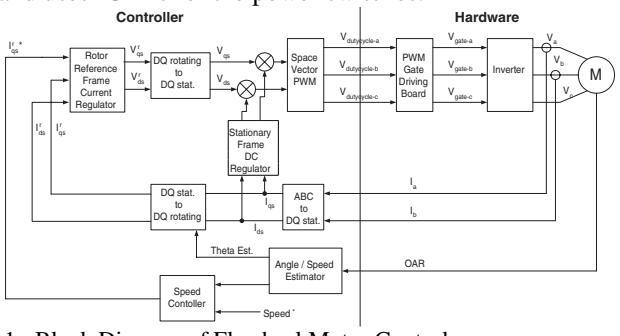

Figure 1: Block Diagram of Flywheel Motor Control

The control room has independent stations for various functions: magnetic bearing control, motor control, dc power supply control and temperature monitoring. The motor control function is implemented digitally using a commercially available microprocessor board. The control algorithms are written in a high level block diagram simulation language and converted to the necessary microprocessor code via software provided by the manufacturer of the microprocessor board. The motor current is measured in the test cell and fed back to an analog to digital (A/D) converter board in the control room. The inverter power switch duty cycles are calculated digitally as part of the control algorithm and output as analog signals using a digital to analog (D/A) converter. The duty cycle analog signals are sent to a pulse width modulation (PWM) generation board in the test cell. The output of the PWM generation board is a set of gate drive signals for the inverter unit. A block diagram of the motor control is shown in Figure 1 and described extensively in the next section.

MOTOR CONTROL ALGORITHM

The motor control algorithm is based on the principles of field orientation control or "vector control" [1]. The basic idea behind this control technique is to orient the applied stator currents to the rotor magnetic field. When this is done, the motor control is simplified because the control variables become dc quantities in steady state. The operating point of the machine can then be accurately and dynamically controlled so that high efficiency and fast response are obtained. A brief mathematical description for this technique follows.

A three phase machine, without a neutral connection, can be equivalently described as a two phase machine through a transformation from abc coordinates to dq coordinates as follows [2].

$$f_q = f_a \tag{1}$$

$$f_d = -\frac{1}{\sqrt{3}} f_a - \frac{2}{\sqrt{3}} f_b \tag{2}$$

The reverse transformation is

$$f_a = f_q \tag{3}$$

$$f_b = -\frac{1}{2} f_q - \frac{\sqrt{3}}{2} f_d \tag{4}$$

$$f_c = -\frac{1}{2} f_q + \frac{\sqrt{3}}{2} f_d \tag{5}$$

The d and q variables described in (1) and (2) are in the stator reference frame. From (1) it can be seen that the q-axis is aligned with the 'a' phase. This means that the 'a' phase current is equal to the q-axis current and the 'a' phase voltage (V_{an}) is equal to the q-axis voltage.

In a permanent magnetic machine, it is convenient to transform these variables to a reference frame that is rotating synchronously with the rotor magnetic field. In the rotor reference frame, the d-axis is defined to be co-linear with the rotor magnetic field axis. The transformation from the stator frame to the rotor frame is given by (6) and the inverse transformation is given by (7) [2].

$$\begin{bmatrix} f_q^r \\ f_d^r \end{bmatrix} = \begin{bmatrix} \cos\theta_r & -\sin\theta_r \\ \sin\theta_r & \cos\theta_r \end{bmatrix} \begin{bmatrix} f_q^s \\ f_d^s \end{bmatrix} \tag{6}$$

$$\begin{bmatrix} f_q^s \\ f_d^s \end{bmatrix} = \begin{bmatrix} \cos\theta_r & \sin\theta_r \\ -\sin\theta_r & \cos\theta_r \end{bmatrix} \begin{bmatrix} f_q^r \\ f_d^r \end{bmatrix} \tag{7}$$

The permanent magnetic synchronous machine can then be modeled in the rotor reference frame as follows [1]. Equation (9) gives the stator flux linkages in the rotor reference frame and (10) is the torque expression.

$$\begin{bmatrix} V_{qs}^r \\ V_{ds}^r \end{bmatrix} = \begin{bmatrix} R_s + L_q p & \omega_r L_d \\ -\omega_r L_q & R_s + L_d p \end{bmatrix} \begin{bmatrix} i_{qs}^r \\ i_{ds}^r \end{bmatrix} + \begin{bmatrix} \omega_r \lambda_{af} \\ 0 \end{bmatrix} \tag{8}$$

$$\begin{bmatrix} \lambda_{qs}^r \\ \lambda_{ds}^r \end{bmatrix} = \begin{bmatrix} L_q & 0 \\ 0 & L_d \end{bmatrix} \begin{bmatrix} i_{qs}^r \\ i_{ds}^r \end{bmatrix} + \begin{bmatrix} 0 \\ \lambda_{af} \end{bmatrix} \tag{9}$$

$$T_e = \frac{3P}{4} \left[\lambda_{ds}^r i_{qs}^r - \lambda_{qs}^r i_{ds}^r \right] \tag{10}$$

In field orientation control the d-axis current, i_{ds}^r, is commanded to 0. From (9) and (10) it can be seen that this results in a simplified expression for torque, given in (11).

$$T_e = \frac{3P}{4} \left[\lambda_{af} i_{qs}^r \right] \tag{11}$$

Because the magnitude of λ_{af} is constant due to the rotor magnets, the torque of the machine is proportional to the q-axis current. This result is similar to the dc motor with a constant field winding current where the torque is equal to the armature current times the torque constant. Thus control of the torque is achieved by properly controlling the rotor reference frame currents, i_{qs}^r and i_{ds}^r.

The torque command to the machine is determined from the outer loop control. In the results presented here, the outer loop is a speed controller, that is, errors in speed result in a correcting torque command. In an actual flywheel energy storage system, the torque command is derived from dc bus current or voltage commands. This is described in a companion paper [3].

To control the currents in the machine to be the commanded values, a current regulated voltage source inverter is used. This means that current errors result in voltage commands to the inverter which increase or decrease the applied voltage to increase or decrease the current respectively. This is accomplished through a synchronous frame current regulator [4] that is basically a PI controller operating on the rotor reference frame currents. The output of the controller is considered to be a voltage command in the rotor reference frame that is then transformed to the stator reference frame. The stator frame voltage commands are then used to calculate the inverter switch duty cycles.

There are several methods to find the duty cycles from the commanded stator frame voltages [5]. In the implementation used here, space vector modulation is used. Space vector modulation is a digital technique to calculate the duty cycles directly from the stator reference frame d and q voltages. One advantage of space vector modulation is that it increases the dc bus utilization to the maximum value. This means that for a given dc bus voltage, the maximum fundamental phase voltage is achievable by using space vector modulation. This is in contrast to the more common sine-triangle modulation which results in a lower dc bus utilization.

In this implementation, the duty cycles are output as analog signals which are sent to a PWM generation board. The analog signals are compared to a carrier signal triangle wave to create the gate drive signals to the inverter. This method allows the switching frequency to be separate from the sample frequency which is limited by the calculation time of the

control algorithm. In this implementation, the sample time is set to 100 usec and the PWM switching frequency is set to twice that value at 20 kHz which is the maximum switching frequency of the inverter.

It can be seen by the rotor reference frame transformations of (6) and (7) that the rotor reference frame quantities are based on the rotor angle, θ_r. Thus it is necessary to know what this angle is. In industrial implementations of field orientation, it is common to use an encoder or resolver to feed back the rotor position. The high speed nature of this application makes it difficult to use the traditional feedback devices. Instead, the rotor position is estimated based on knowledge of a "once around" (OAR) position marker. In this machine, one half of the rotor hub is coated with a dark oxide, the other half is polished aluminum. The once around signal is based on the optical detection of the dark or light surface and thus a square wave at the same frequency as the machine speed is generated with the rising edge corresponding to the change from dark oxide to polished aluminum. Due to the large inertia of the flywheel rotor, the speed is reasonably assumed to be constant between once around signals and from this, the position can be estimated. This will be discussed further in the next section.

INITIAL IMPLEMENTATION ISSUES

Back EMF Test

As explained previously, to properly control the motor using the field orientation technique, the instantaneous position of the rotor q-axis with respect to the stator q-axis (θ_r) must be known. The once around signal indicates the position of the color change (dark to light) on the rotor but this does not necessarily coincide with the position of the rotor q-axis. What needs to be determined is the angle between the rotor q-axis and the stator q-axis as a function of the once around signal. This can be determined experimentally by measuring both the phase voltages of the machine and the once around signal as the rotor freely decelerates ("spins down"). For a freely decelerating machine, the stator current is 0 so the phase voltages are entirely due to the back emf of the machine. Stated mathematically, (for 0 stator current) [1]:

$$V_{qs}^{s} = p\lambda_{qs}^{s} \text{ where } \lambda_{qs}^{s} = \lambda_{af}\sin(\theta_r) \quad (12)$$

$$V_{ds}^{s} = p\lambda_{ds}^{s} \text{ where } \lambda_{ds}^{s} = \lambda_{af}\cos(\theta_r) \quad (13)$$

By definition, $V_{qs}^{s}=V_{an}$ because the q-axis in the transformation of (1) is aligned with the stator a-phase. Thus in a freely decelerating machine, the relationship between θ_r and V_{an} is given in (14).

$$V_{an} = \lambda_{af}\cos(\theta_r) \quad (14)$$

V_{an} can be measured if there is a neutral terminal on the machine or V_{ab} can be measured and V_{an} calculated. In this case, the motor neutral was available for measurement purposes (not normally connected). Figure 2 shows a plot of the once around signal and the V_{an} voltage.

From (14) it can be seen that when $\theta_r = 0$, V_{an} will be at a maximum. Figure 2 shows that this maximum occurs twice in one cycle of the OAR signal at approximately the middle of each pulse. The machine is a 4 pole machine so between every rising edge of the OAR signal, 360 mechanical and 720 electrical degrees will have passed. Figure 2 shows that the V_{an} maximum occurs approximately 90 mechanical degrees or 180 electrical degrees behind the rising edge of the OAR signal. This means that the θ_r transformation angle is equal to the electrical angle determined by the OAR signal minus 180º.

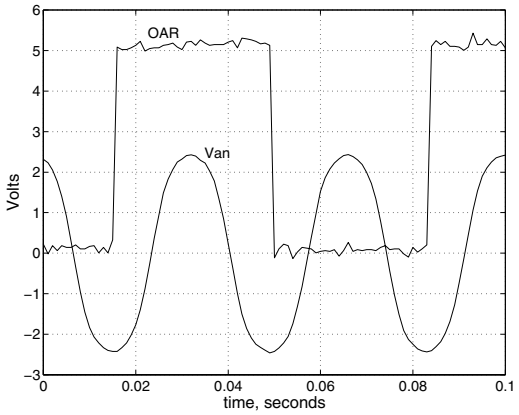

Figure 2: Phase voltage and OAR signal for freely decelerating rotor.

Once the relationship between θ_r and the once around signal is known, the transformation from the stator to the rotor reference frame can be done. From (8), it can be seen that for a freely decelerating rotor, when $i_{qs}^{r} = i_{ds}^{r} = 0$, the back emf voltage appears entirely in the rotor reference frame q-axis and $V_{ds}^{r} = 0$. This means that the transformation angle θ_r can be fine-tuned. The voltages measured in the back emf test can be transformed to the rotor reference frame using the relationship

$$\theta_r = \text{OAR electrical angle - } 180º. \quad (15)$$

If the transformation angle θ_r given by (15) is not exactly correct, then V_{ds}^{r} will not be exactly zero. Figure 3 shows a plot of V_{ds}^{r} where θ_r lags the OAR electrical angle by 180º. It can be seen that V_{ds}^{r} is slightly less than zero. Figure 3 also shows the case where θ_r lags the OAR electrical angle by 170º. It can be seen that this average value of V_{ds}^{r} is now more nearly equal to zero. Thus the actual transformation angle used in the control algorithm is given by (16).

$$\theta_r = \text{OAR electrical angle- } 170º \text{ degrees} \quad (16)$$

The ac components of the q and d axis voltages in Fig. 3 are due to the spatial harmonics of the motor windings and are

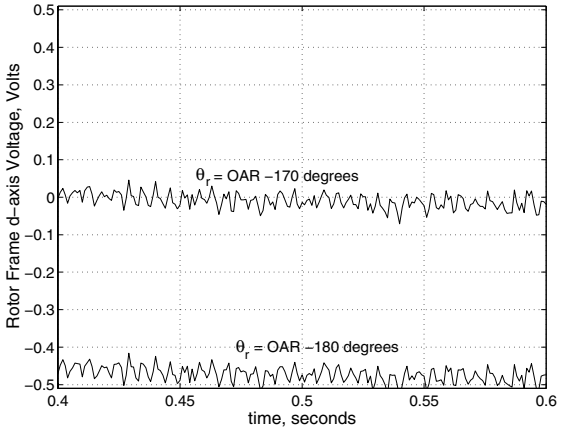

Figure 3: V_{ds}^{r} for Variations in θ_r.

Starting the machine

To operate the machine using field orientation, the rotor position angle must be known. However, the machine must be spinning to estimate the position from the once around position. Initially, this dilemma was resolved by starting the machine in "open loop" operation. A fixed voltage and frequency were applied to the machine directly until the rotor started to move. Once a OAR signal was established, the control of the machine was shifted to closed loop speed control.

It was additionally observed that the machine could start under closed loop control if a low speed command was given.

EXPERIMENTAL RESULTS

Closed Speed Loop Operation

Closed loop speed control was achieved by using a PI loop around the torque control as shown in Fig. 1 and the unit was tested at speeds up to 20,000 rpm. Using the once around signal, two methods were developed to estimate the speed and position. The first method works well at low speeds and degrades as the speed increases due to quantization errors. The second method is limited at low speeds due to saturation of the digital counter register but works very well at high speeds.

Speed Estimate: Method One

In this method, the speed was determined by counting the number of sample periods, t_p, between once around signals and multiplying by the sample rate, T_s as shown in (17). The speed was assumed to be constant between OAR signals leading to the position estimate shown in (18) where t_{pz} is the number of sample periods since the last rising edge of the OAR signal. The position estimate was reset to zero at every rising edge of the OAR signal.

$$\text{Speed}_{\text{rpm}} = \frac{60}{t_p T_s}. \tag{17}$$

$$\theta_{\text{electrical}}{}^{\text{rad}} = \text{Speed}_{\text{rpm}} \frac{2\pi}{30} t_{pz} \tag{18}$$

The sample rate of the control algorithm is 100 usec. This leads to the possibility of error shown in Table 1. The quantization errors of this method led to speed oscillations which became progressively worse as the speed increased. Figure 4 shows the speed estimate for a commanded speed of 5000 rpm. Oscillations on the order of 12 rpm are clearly evident. Figure 5 shows the impact of the speed oscillations on the phase current.

Actual Machine Speed (rpm)	Maximum Possible Speed Estimate Error, Method One, rpm	Maximum Possible Speed Estimate Error, Method Two, rpm
1,000	1.66	.03
5,000	41.32	.83
10,000	163.93	3.33
20,000	645.16	13.32
60,000	5454.54	119.76

Table 1: Possible Speed Errors for Alternate Methods

Speed Estimate: Method Two

This method was based on a commercially available timer board which contains two 16 bit counters. Counter 1 is used to determine the OAR frequency and counter 2 is used to determine the time that has elapsed since the most recent rising edge of the OAR signal. The counter clocks are scaled so that a signal in the range of 7.64 Hz to 500 kHz may be detected. (The clock rates may be scaled higher in software as necessary for higher rotor speeds.) The speed is determined from counter 1 and (19) and the OAR electrical angle is determined from (20) where 'f' is the output of counter 1 and 't' is the output of counter 2.

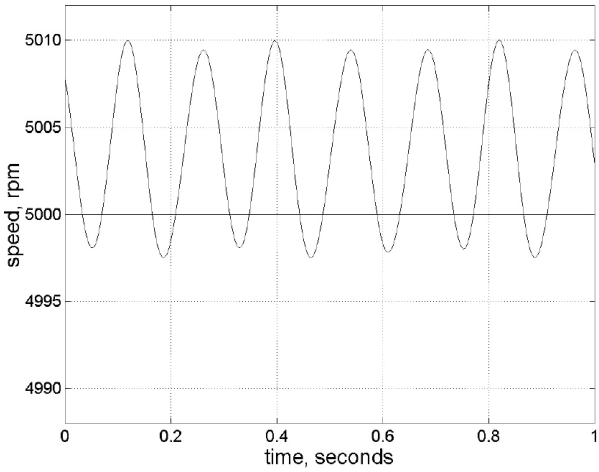

Figure 4: Speed Oscillation due to Quantization Error with Method One Speed Estimate

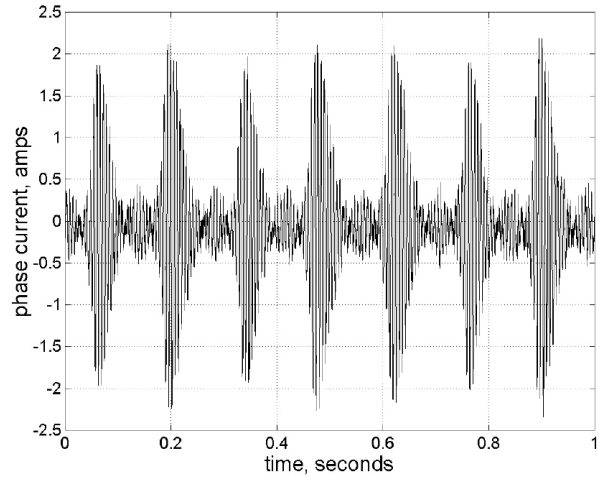

Figure 5: Oscillations in Phase Current due to Speed Estimate Oscillations for Method Two

$$\text{Speed}_{\text{rpm}} = 60 \frac{f}{2} \tag{19}$$

$$\theta_{\text{electrical}}{}^{\circ} = 4\pi f t \tag{20}$$

The motor speed using speed estimate method two for feedback is shown in Fig. 6. The oscillations in both the speed estimate and the phase current (Fig. 7) are eliminated.

DC Offset Currents

Figure 8 shows the frequency spectrum of the phase current at an operating speed of 10,000 rpm. The fundamental component, at 333 Hz, clearly dominates. However, there is a significant dc component also present. Although not predicted theoretically, the dc component may be caused by slight

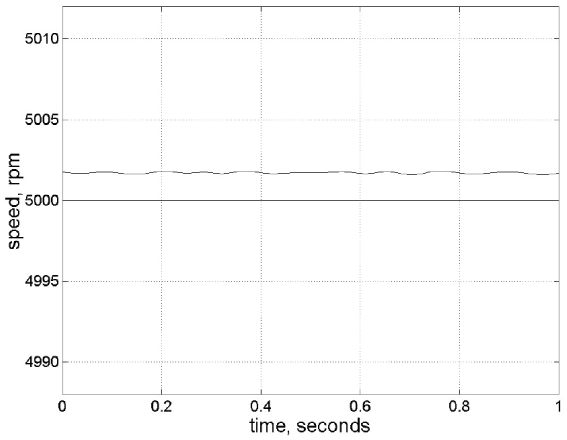

Figure 6: Speed oscillation with Method Two Speed Estimate

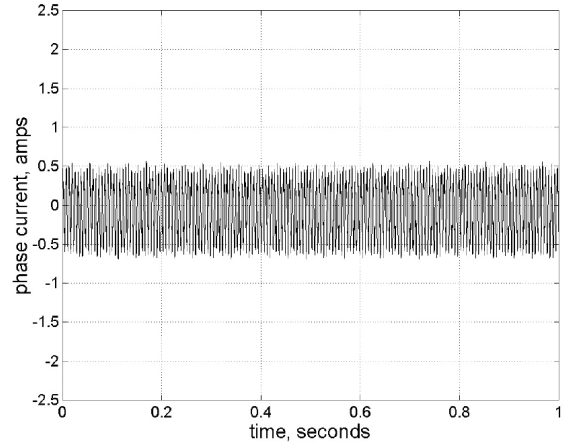

Figure 7: Phase Current with Method Two Speed Estimate

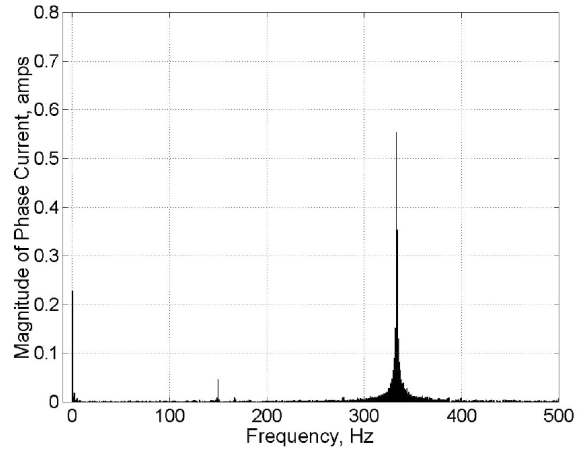

Figure 8: Phase Current Frequency Spectrum at 10,000 rpm

mismatches or offsets in the phase voltages applied to the machine.

The synchronous frame current regulator was tuned for a bandwidth of 200 Hz. The synchronous electrical speed at 10,000 rpm is 333 Hz. This means that currents in the frequency range of 133 Hz to 533 Hz are within the bandwidth of the current regulator. Thus the current regulator will not effectively eliminate the dc currents. One approach to this problem is to introduce an additional current regulator which operates in the stationary reference frame. This current regulator is a PI controller tuned to have a very low bandwidth so it essentially only regulates the dc current as shown in Fig. 9. Due to the low bandwidth of the PI, the fundamental current passes through the regulator unchanged while the dc current is regulated to zero. Using the stationary frame current regulator in addition to the synchronous frame current regulator resulted in the elimination of the dc component as shown in Fig. 10.

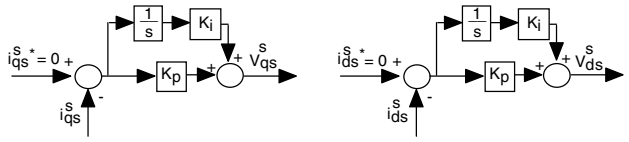

Figure 9: Block Diagrams of d- and q-axis Stationary Frame DC Current Regulators

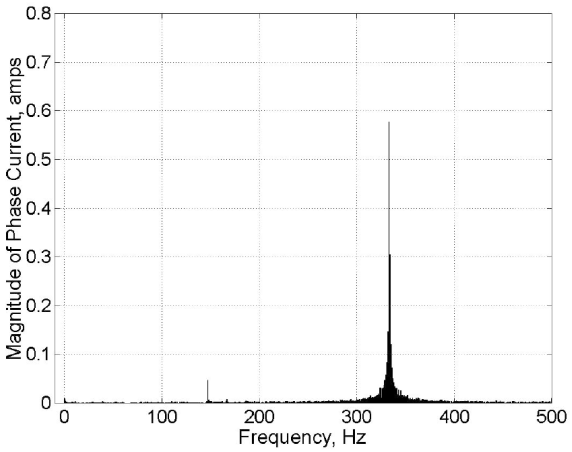

Figure 10: Phase Current Frequency Spectrum at 10,000 rpm with stationary frame current regulator

Sensitivity to Error in Position Estimate

In this implementation of field orientation control the commanded d-axis current, i^r_{ds}, is set equal to zero. In this strategy, the direct axis stator flux linkage, λ^r_{ds}, is constant and due entirely to the rotor magnet with no contribution from the stator current. The torque is produced by the interaction of this flux with the q-axis current according to (11). However, if the rotor reference frame transformation angle, θ_r, is not correct, then there will be d-axis current in addition to the commanded q-axis current. For small errors in angle estimate, this additional current does not contribute significantly to the total phase current in the machine. However, as the error approaches 90 electrical degrees, the theoretical maximum, the total stator current increases rapidly. This is shown in Fig. 11. The data points in Fig. 11 were taken at a speed of 7,000 rpm.

20000 RPM OPERATION

The speed of the motor was limited to 20,000 rpm due to limits on the particular flywheel rotor used in the system. The following results show steady state operation at 20,000 rpm. The small magnitude of the phase current (rms value just over 1 amp) indicates the very low losses of the machine when suspended on magnetic bearings and operated in a vacuum. Fig. 12 shows the motor phase current. The current looks

somewhat distorted however an examination of the spectrum shown in Fig. 13 shows the major frequency component at 667 Hz as expected. Also, the current shown in Fig. 12 has an extremely small magnitude which may contribute to the perceived distortion.

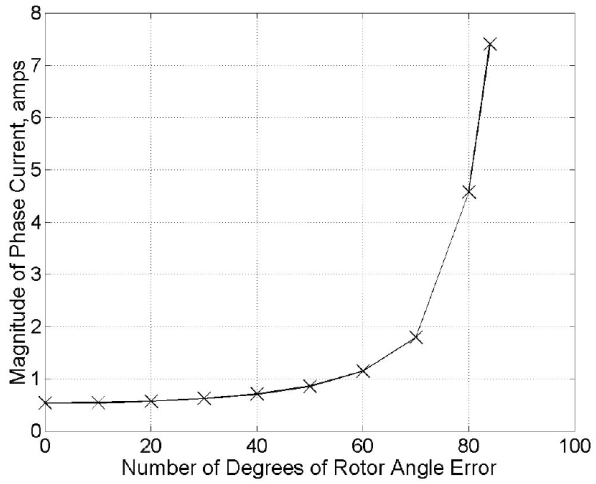

Figure 11: Sensitivity of Phase Current to Rotor Angle Error

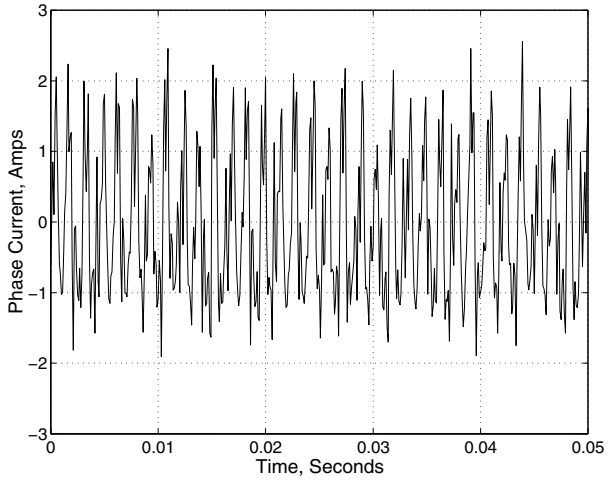

Figure 12: Motor Phase Current at 20,000 rpm Operation

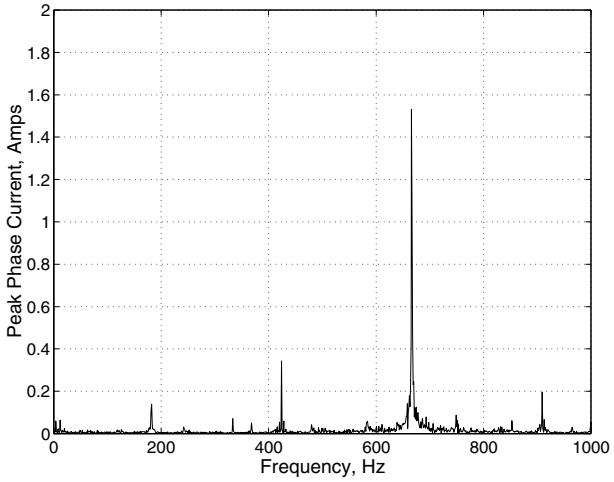

Figure 13: Motor Phase Current Spectra for 20,000 rpm Operation

Finally, Fig. 14 shows the duty cycle for the phase A high switch at 20,000 rpm with a 120 volt dc bus for both sine-triangle modulation and space vector modulation. This plot shows that the space vector modulation technique needs less dc bus voltage than the sine-triangle technique to generate the same phase voltage. The space vector duty cycle is seen to be well within the duty cycle range of zero to one for operation at this speed from this voltage. However, the duty cycle for the sine-triangle technique is clamped at one at some points and at zero at others. This duty cycle which would result in a higher distortion of the synthesized phase voltage.

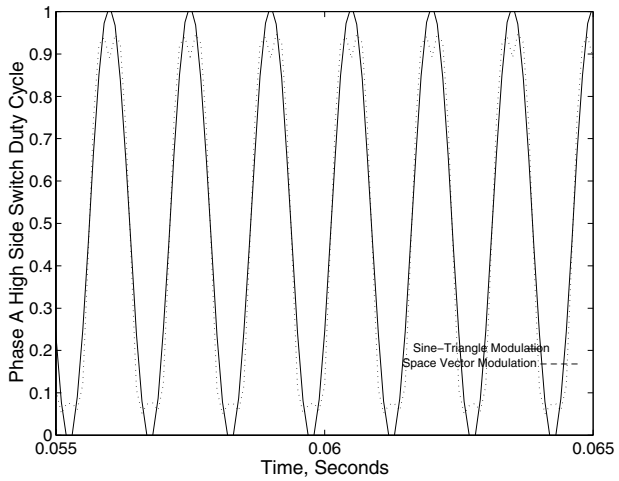

Figure 14: Phase A High Switch Duty Cycle for Space Vector Modulation and for Sine-Triangle Modulation

CONCLUSIONS

This paper has presented the initial experimental results of the flywheel motor test facility at the NASA Glenn Research Center. The once around signal was successfully used for speed and position feedback. The back emf test and the subsequent fine-tuning was shown to accurately determine the relationship between the OAR and the rotor q-axis. The dc offset current was eliminated with the addition of the concurrent stationary frame regulator. Space vector modulation was shown to increase the dc bus utilization over sine-triangle modulation.

REFERENCES

[1] Krishnan, Ramu, *Permanent Magnet Synchronous and Brushless DC Motor Drives: Theory, Operation, Performance, Modeling, Simulation, Analysis and Design*, Virginia Tech., Blacksburg, Virginia, 1999.

[2] Krause, Paul, *Analysis of Electric Machinery*, McGraw-Hill Book Company, New York, New York, 1986.

[3] Kascak, P., B. Kenny, W. Santiago, R. Jansen, T. Dever "International Space Station (ISS) Bus Regulation Studies with NASA Glenn Research Center (GRC) Flywheel Energy Storage System Development Unit*", to be published at 2001 IECEC*, Savannah, Georgia.

[4] Rowan, T. and R. Kerkman, "A New Synchronous Current Regulator and an Analysis of Current-Regulated PWM Inverters", *IEEE Transactions on Industry Applications*, Vol IA-22, No. 4, July/August 1986, pp. 678-690.

[5] Holtz, Joachim, "Pulsewidth Modulation for Electronic Power Conversion*", Proceedings of the IEEE*, Volume 82, No. 8, August, 1994, pp. 1194-1214.

REPORT DOCUMENTATION PAGE

Form Approved
OMB No. 0704-0188

1. AGENCY USE ONLY (*Leave blank*)	2. REPORT DATE	3. REPORT TYPE AND DATES COVERED
	July 2001	Technical Memorandum

4. TITLE AND SUBTITLE

Advanced Motor Control Test Facility for NASA GRC Flywheel Energy Storage System Technology Development Unit

5. FUNDING NUMBERS

WU–755–84–09–00

6. AUTHOR(S)

Barbara H. Kenny, Peter E. Kascak, Heath Hofmann, Michael Mackin, Walter Santiago, and Ralph Jansen

7. PERFORMING ORGANIZATION NAME(S) AND ADDRESS(ES)

National Aeronautics and Space Administration
John H. Glenn Research Center at Lewis Field
Cleveland, Ohio 44135–3191

8. PERFORMING ORGANIZATION REPORT NUMBER

E–12840

9. SPONSORING/MONITORING AGENCY NAME(S) AND ADDRESS(ES)

National Aeronautics and Space Administration
Washington, DC 20546–0001

10. SPONSORING/MONITORING AGENCY REPORT NUMBER

NASA TM—2001-210986
IECEC2001–AT–11

11. SUPPLEMENTARY NOTES

Prepared for the 36th Intersociety Energy Conversion Engineering Conference cosponsored by the ASME, IEEE, AIChE, ANS, SAE, and AIAA, Savannah, Georgia, July 29–August 2, 2001. Barbara H. Kenny, Michael Mackin, and Walter Santiago, NASA Glenn Research Center; Peter E. Kascak and Ralph Jansen, Ohio Aerospace Institute, 22800 Cedar Point Road, Brook Park, Ohio 44142; and Heath Hofmann, Department of Electrical Engineering, Pennsylvania State University, University Park, Pennsylvania 16802. Responsible person, Barbara H. Kenny, organization code 5450, 216–433–6289.

12a. DISTRIBUTION/AVAILABILITY STATEMENT

Unclassified - Unlimited
Subject Categories: 20 and 33 Distribution: Nonstandard

Available electronically at http://gltrs.grc.nasa.gov/GLTRS

This publication is available from the NASA Center for AeroSpace Information, 301–621–0390.

12b. DISTRIBUTION CODE

13. ABSTRACT ***(Maximum 200 words)***

This paper describes the flywheel test facility developed at the NASA Glenn Research Center with particular emphasis on the motor drive components and control. A 4-pole permanent magnet synchronous machine, suspended on magnetic bearings, is controlled with a field orientation algorithm. A discussion of the estimation of the rotor position and speed from a "once around signal" is given. The elimination of small dc currents by using a concurrent stationary frame current regulator is discussed and demonstrated. Initial experimental results are presented showing the successful operation and control of the unit at speeds up to 20 000 rpm.

14. SUBJECT TERMS

Flywheel energy storage; Permanent magnet synchronous machine; Motor drives; Field orientation control

15. NUMBER OF PAGES

12

16. PRICE CODE

17. SECURITY CLASSIFICATION OF REPORT	18. SECURITY CLASSIFICATION OF THIS PAGE	19. SECURITY CLASSIFICATION OF ABSTRACT	20. LIMITATION OF ABSTRACT
Unclassified	Unclassified	Unclassified	